

Particle acceleration mechanisms

V. Petrosian · A.M. Bykov

Received: 22 November 2007; Accepted: 14 december 2007

Abstract In this paper we review the possible mechanisms for production of non-thermal electrons which are responsible for the observed non-thermal radiation in clusters of galaxies. Our primary focus is on non-thermal Bremsstrahlung and inverse Compton scattering, that produce hard X-ray emission. We first give a brief review of acceleration mechanisms and point out that in most astrophysical situations, and in particular for the intracluster medium, shocks, turbulence and plasma waves play a crucial role. We also outline how the effects of the turbulence can be accounted for. Using a generic model for turbulence and acceleration, we then consider two scenarios for production of non-thermal radiation. The first is motivated by the possibility that hard X-ray emission is due to non-thermal Bremsstrahlung by nonrelativistic particles and attempts to produce non-thermal tails by accelerating the electrons from the background plasma with an initial Maxwellian distribution. For acceleration rates smaller than the Coulomb energy loss rate, the effect of energising the plasma is to primarily heat the plasma with little sign of a distinct non-thermal tail. Such tails are discernible only for acceleration rates comparable or larger than the Coulomb loss rate. However, these tails are accompanied by significant heating and they are present for a short time of $< 10^6$ yr, which is also the time that the tail will be thermalised. A longer period of acceleration at such rates will result in a runaway situation with most particles being accelerated to very high energies. These more exact treatments confirm the difficulty with this model, first pointed out by Petrosian (2001). Such non-thermal tails, even if possible, can only explain the hard X-ray but not the radio emission which needs GeV or higher energy electrons. For these and for production of hard X-rays by the inverse Compton model, we need the second scenario where there is injection and subsequent acceleration of relativistic electrons. It is shown that a steady state situation, for example arising from secondary electrons produced from cosmic ray proton scattering by background protons, will most likely lead to flatter than required electron spectra or it

V. Petrosian
Department of Physics, Stanford University, Stanford, CA 94305
E-mail: vahep@stanford.edu

A.M. Bykov
A.F. Ioffe Institute for Physics and Technology, St. Petersburg, 194021, Russia
E-mail: byk@astro.ioffe.ru

requires a short escape time of the electrons from the cluster. An episodic injection of relativistic electrons, presumably from galaxies or AGN, and/or episodic generation of turbulence and shocks by mergers can result in an electron spectrum consistent with observations but for only a short period of less than one billion years.

Keywords intergalactic medium · particle acceleration · galaxies: clusters: general

1 Introduction

In this paper we attempt to constrain the acceleration models based on the observations described in the papers by Durret et al. (2008), Rephaeli et al. (2008) and Ferrari et al. (2008) - Chapters 4 – 6, this volume, and the required spectrum of the accelerated electrons shown in Fig. 6 of Petrosian et al. 2008 - Chapter 10, this volume. However, before addressing these details we first compare various acceleration processes and stress the importance of plasma waves or turbulence (PWT) as an agent of scattering and acceleration, and then describe the basic scenario and equations for treatment of these processes. As pointed out below there is growing evidence that PWT plays an important role in acceleration of particles in general, and in clusters of galaxies in particular. The two most commonly used acceleration mechanisms are the following.

1.1 Electric field acceleration

Electric fields parallel to magnetic fields can accelerate charged particles and can arise as a result of magnetic field reconnection in a current sheet or other situations. For fields less than the so-called Dreicer field, defined as $E_D = kT/(e\lambda_{\text{Coul}})$, where

$$\lambda_{\text{Coul}} \sim 15 \text{ kpc} \left(\frac{T}{10^8 \text{ K}} \right)^2 \left(\frac{10^{-3} \text{ cm}^{-3}}{n} \right) \quad (1)$$

is the collision (electron-electron or proton-proton) mean free path¹, the rate of acceleration is less than the rate of collision losses and only a small fraction of the particles can be accelerated into a non-thermal tail of energy $E < LeE_D$. For the ICM $E_D \sim 10^{-14} \text{ V cm}^{-1}$ and $L \sim 10^{24} \text{ cm}$ so that sub-Dreicer fields can only accelerate particles up to 100's of keV, which is far below the 10's of GeV electrons required by observations. Super-Dreicer fields, which seem to be present in many simulations of reconnection (Drake, 2006; Cassak et al., 2006; Zenitani & Hoshino, 2005), accelerate particles at a rate that is faster than the collision or thermalisation time τ_{therm} . This can lead to a runaway and an unstable electron distribution which, as shown theoretically, by laboratory experiments and by the above mentioned simulations, most probably will give rise to PWT (Boris et al., 1970; Holman, 1985).

In summary the electric fields arising as a result of reconnection cannot be the sole agent of acceleration in the ICM, because there are no large scale magnetically dominated cosmological flows, but it may locally produce an unstable particle momentum distribution which will produce PWT that can then accelerate particles.

¹ The proton-proton or ion-ion mean free path will be slightly smaller because of the larger value of the Coulomb logarithm $\ln A \sim 40$ in the ICM.

1.2 Fermi acceleration

Nowadays this process has been divided into two kinds. In the original Fermi process particles of velocity v moving along magnetic field lines (strength B) with a pitch angle $\cos \mu$ undergo random scattering by moving agents with a velocity u . Because the head (energy gaining) collisions are more probable than trailing (energy losing) collisions, on average, the particles gain energy at a rate proportional to $(u/v)^2 D_{\mu\mu}$, where $D_{\mu\mu}$ is the pitch angle diffusion rate. This, known as a *second order Fermi process* is what we shall call stochastic acceleration. In general, the most likely agent for scattering is PWT. An alternative process is what is commonly referred to as a *first order Fermi process*, where the actual acceleration occurs when particles cross a shock or any region of converging flow. Upon crossing the shock the fractional gain of momentum $\delta p/p \propto u_{\text{sh}}/v$. Ever since the 1970's, when several authors demonstrated that a very simple version of this process leads to a power law spectrum that agrees approximately with observations of the cosmic rays, shock acceleration is commonly invoked in space and astrophysical plasmas. However, this simple model, though very elegant, has some shortcomings specially when applied to electron acceleration in non-thermal radiating sources. Moreover, some of the features that make this scenario for acceleration of cosmic rays attractive are not present in most radiating sources where one needs efficient acceleration of electrons to relativistic energies from a low energy reservoir.

The original, test particle theory of diffusive shock acceleration (DSA), although very elegant and independent of geometry and other details (e.g. Blandford & Ostriker 1978) required several conditions such as injection of seed particles and of course turbulence. A great deal of work has gone into addressing these aspects of the problem and there has been a great deal of progress. It is clear that nonlinear effects (see e.g. Drury 1983; Blandford & Eichler 1987; Jones & Ellison 1991; Malkov & Drury 2001) and losses (specially for electrons) play an important role and modify the resultant spectra and efficiency of acceleration. Another important point is the source of the turbulence or the scattering agents. A common practice is to assume Bohm diffusion (see e.g. Ellison et al. 2005). Second order acceleration effects could modify the particle spectra accelerated by shocks (see e.g. Schlickeiser et al. 1993; Bykov et al. 2000). Although there are indications that turbulence may be generated by the shocks and the accelerated particle upstream, many details (e.g. the nature and spectrum of the turbulence) need to be addressed more quantitatively. There has been progress on the understanding of generation of the magnetic field and turbulence on strong shocks (Bell & Lucek, 2001; Amato & Blasi, 2006; Vladimirov et al., 2006) as required in recent observations of supernova remnants (see e.g. Völk et al. 2005). There is also some evidence for these processes from observations of heliospheric shocks (see e.g. Kennel et al. 1986; Ellison et al. 1990). Basic features of particle acceleration by cosmological shocks were discussed by Bykov et al. 2008a - Chapter 7, this volume, so we will concentrate here on the stochastic acceleration perspective.

1.3 Stochastic acceleration

The PWT needed for scattering can also accelerate particles stochastically with a rate D_{EE}/E^2 , where D_{EE} is the energy diffusion coefficient, so that shocks may not be always necessary. In low beta plasmas, $\beta_p = 2(v_s/v_A)^2 < 1$, where the Alfvén velocity

$v_A = \sqrt{B^2/4\pi\rho}$, the sound velocity $v_s = \sqrt{kT/m}$, $\rho = nm$ is the mass density and n is the number density of the gas, and for relativistic particles the PWT-particle interactions are dominated by Alfvénic turbulence, in which case the rate of energy gain $D_{EE}/E^2 = (v_A/v)^2 D_{\mu\mu} \ll D_{\mu\mu}$, so that the first order Fermi process is more efficient. However, at low energies and/or in very strongly magnetised plasmas, where v_A can exceed c , the speed of light², the acceleration rate may exceed the scattering rate (see Pryadko & Petrosian 1997), in which case low energy electrons are accelerated more efficiently by PWT than by shocks.³

Irrespective of which process dominates the particle acceleration, it is clear that PWT has a role in all of them. Thus, understanding of the production of PWT and its interaction with particles is extremely important. Moreover, turbulence is expected to be present in most astrophysical plasmas including the ICM and in and around merger or accretion shocks, because the ordinary and magnetic Reynolds numbers are large. Indeed turbulence may be the most efficient channel of energy dissipation. In recent years there has been a substantial progress in the understanding of MHD turbulence (Goldreich & Sridhar, 1995, 1997; Lithwick & Goldreich, 2003; Cho & Lazarian, 2002, 2006). These provide new tools for a more quantitative investigation of turbulence and the role it plays in many astrophysical sources.

2 Turbulence and stochastic acceleration

2.1 Basic scenario

The complete picture of stochastic acceleration by PWT is a complex and not yet fully understood or developed process. However, one might envision the following scenario.

Turbulence or plasma waves can be generated in the ICM on some macroscopic scale $L \sim 300$ kpc (some fraction of the cluster size or some multiple of galactic sizes) as a result of merger events or by accretion or merger shocks. That these kind of motions or flows with velocity comparable to or somewhat greater than the virial velocity $u_L \sim 1000$ km s⁻¹ will lead to PWT is very likely, because in the ICM the ordinary Reynolds number $Re = u_L L/\nu \gg 1$. Here $\nu \sim v_{th} \lambda_{scat}/3$ is the viscosity, $v_{th} = \sqrt{kT/m} \sim u_L (T/10^8)^{1/2}$ and λ_{scat} is the mean free path length. The main uncertainty here is in the value of λ_{scat} . For Coulomb collisions $\lambda_{scat} \sim 15$ kpc (Eq. 1) and $Re \sim 100$ is just barely large enough for generation of turbulence. However, in a recent paper Brunetti & Lazarian (2007) argue that in the presence of a magnetic field of $B \sim \mu\text{G}$, $v_A \sim 70(B/\mu\text{G})(10^{-3} \text{ cm}^{-3}/n)^{1/2}$ km s⁻¹ is much smaller than v_{th} so that the turbulence will be super-Alfvénic, in which case the mean free path may be two orders of magnitude smaller⁴ yielding $Re \sim 10^4$. We know this also to be true from a phenomenological consideration. In a cluster the hot gas is confined by the gravitational field of the total (dark and ‘visible’) matter. Relativistic particles, on the other hand, can cross the cluster of radius R on a timescale of $T_{cross} = 3 \times 10^6 (R/\text{Mpc})$ yr and can escape the cluster (see Fig. 4 below), unless confined by a chaotic magnetic field or a scattering agent such as turbulence with a mean free path $\lambda_{scat} \ll R$. If so,

² Note that the Alfvén group velocity $v_g = c\sqrt{v_A^2/(v_A^2 + c^2)}$ is always less than c .

³ In practice, i.e. mathematically, there is little difference between the two mechanisms (Jones, 1994), and the acceleration by turbulence and shocks can be combined (see below).

⁴ Plasma instabilities, possibly induced by the relativistic particles, can be another agent of decreasing the effective particle mean free path (Schekochihin et al., 2005).

then the escape time $T_{\text{esc}} \sim T_{\text{cross}}(R/\lambda_{\text{scat}}) = T_{\text{cross}}^2/\tau_{\text{scat}}$. The curve marked with arrows in this figure shows the maximum value of the required τ_{scat} so that the escape time is longer than the energy loss time τ_{loss} . As is evident from this figure, for a GeV electron to be confined for a Hubble timescale, or $T_{\text{esc}} \sim 10^{10}$ yr, we need $\tau_{\text{scat}} \sim 3 \times 10^4$ yr or $\lambda_{\text{scat}} < 10$ kpc. This could be the case in a chaotic magnetic field and/or in the presence of turbulence. Some observations related to this are discussed by Petrosian et al. 2008 - Chapter 10, this volume; see also Vogt & Enßlin (2005). Numerous numerical simulations also agree with this general picture. There is evidence for large scale bulk flows in the simulations of merging clusters (e.g. Roettiger et al. 1996; Ricker & Sarazin 2001), and that these are converted into turbulence with energies that are a substantial fraction of the thermal energy of the clusters (e.g. Sunyaev et al. 2003; Dolag et al. 2005). For more details see Brunetti & Lazarian (2007).

Once the PWT is generated it can undergo two kind of interactions. The first is dissipationless cascade from wave vectors $k_{\text{min}} \sim L^{-1}$ to smaller scales. The cascade is governed by the rates of *wave-wave interactions*. For example, in the case of weak turbulence, that can be considered as a superposition of weakly interacting wave packets, the three wave interactions can be represented as

$$\omega(\mathbf{k}_1) + \omega(\mathbf{k}_2) = \omega(\mathbf{k}_3) \quad \text{and} \quad \mathbf{k}_1 + \mathbf{k}_2 = \mathbf{k}_3, \quad (2)$$

where \mathbf{k} is the wave vector, and the wave frequency, $\omega(\mathbf{k})$, is obtained from the *plasma dispersion relation*. One can interpret Eq. 2 as energy-momentum conservation laws for weakly coupled plasma waves in a close analogy to the optical waves. The interaction rates can be represented by the wave diffusion coefficient D_{ij} or the cascade time $\tau_{\text{cas}} \sim k^2/D_{ij}$. The largest uncertainty is in the diffusion coefficient. Because of the nonlinear nature of the interactions this coefficient depends on the wave spectrum $W(\mathbf{k})$. As mentioned above there has been considerable progress in this area in the past two decades and there are some recipes how to calculate the diffusion coefficients.

The second is **damping of the PWT** by *wave-particle interaction* which terminates the dissipationless cascade, say at an outer scale k_{max} when the damping rate $\Gamma(k_{\text{max}}) = \tau_{\text{cas}}^{-1}(k_{\text{max}})$. The range $k_{\text{min}} < k < k_{\text{max}}$ is called the inertial range. The damping rate can be obtained from the finite temperature dispersion relations (see below). The energy lost from PWT goes into heating the background plasma and/or accelerating particles into a non-thermal tail. These processes are described by the diffusion coefficients D_{EE} and $D_{\mu\mu}$ introduced above. These coefficients are obtained from consideration of the wave-particle interactions which are often dominated by resonant interactions, specially for low beta (magnetically dominated) plasma, such that

$$\omega(\mathbf{k}) - k \cos \theta v \mu = n \Omega / \gamma, \quad (3)$$

for waves propagating at an angle θ with respect to the large scale magnetic field, and a particle of velocity v , Lorentz factor γ , pitch angle $\cos \mu$ and gyrofrequency $\Omega = eB/mc$. Both cyclotron (the term in the right hand side of Eq. 3) and Cerenkov resonance (the second term in the left hand side) play important roles in the analysis (see for details e.g. Akhiezer et al. 1975). Here, when the harmonic number n (not to be confused with the density) is equal to zero, the process is referred to as the *transit time damping*. For gyroresonance damping by waves propagating parallel to the field lines ($\theta = 0$) $n = \pm 1$. For obliquely propagating waves, in principle one gets contributions from all harmonics $n = \pm 1, \pm 2, \dots$, but for practical purposes most of the contribution comes from the lowest harmonics $n = \pm 1$ (see Pryadko & Petrosian 1998).

2.2 Dispersion relations

It is clear from the above description that at the core of the evaluation of wave-wave or wave-particle interactions (and all the coefficients of the kinetic equations described below) lies the plasma dispersion relation $\omega(\mathbf{k})$. It describes the characteristics of the waves that can be excited in the plasma, and the rates of wave-wave and wave-particle interactions.

In the MHD regime for a cold plasma

$$\omega = v_A k \cos \theta \quad \text{and} \quad \omega = v_A k \quad (4)$$

for the Alfvén and the fast (magneto-sonic) waves, respectively. Beyond the MHD regime a multiplicity of wave modes can be present and the dispersion relation is more complex and is obtained from the following expressions (see e.g. Sturrock 1994):

$$\tan^2 \theta = \frac{-P(n_r^2 - R)(n_r^2 - L)}{(Sn_r^2 - RL)(n_r^2 - P)}, \quad (5)$$

where $n_r = kc/\omega$ is the refractive index, $S = \frac{1}{2}(R + L)$, and

$$P = 1 - \sum_i \frac{\omega_{pi}^2}{\omega^2}, \quad R = 1 - \sum_i \frac{\omega_{pi}^2}{\omega^2} \left(\frac{\omega}{\omega + \epsilon_i \Omega_i} \right), \quad \text{and} \quad L = 1 - \sum_i \frac{\omega_{pi}^2}{\omega^2} \left(\frac{\omega}{\omega - \epsilon_i \Omega_i} \right). \quad (6)$$

Here $\omega_{pi}^2 = 4\pi n_i q_i^2/m_i$ and $\Omega_i = |q_i|B/m_i c$ are the plasma and gyro frequencies, $\epsilon_i = q_i/|q_i|$, and n_i , q_i , and m_i are the density, charge, and mass of the background particles. For fully ionised plasmas such as that in the ICM it is sufficient to include terms due to electron, proton and α particles. Fig. 1 shows the dispersion surfaces (depicted by the curves) obtained from the above expressions along with the resonant planes in the $(\omega, k_{\parallel}, k_{\perp})$ space. Intersections between the dispersion surfaces and the resonant planes define the resonant wave-particle interactions and the particle kinetic equation coefficients. One can also envision a similar graphic description of the three wave interactions (Eq. 2) using the intersections of the curved dispersion surfaces. However, such calculations have been carried out only in the MHD regime using the simple relations of Eq. 4, which is already a complicated procedure (see e.g. Chandran 2005; Luo & Melrose 2006).

The above dispersion relations are good approximations for low beta plasmas but in the ICM the plasma beta is large:

$$\beta_p = 8\pi n k T / B^2 = 3.4 \times 10^2 (n/10^{-3} \text{ cm}^{-3}) (\mu G / B)^2 (T/10^8 \text{ K}). \quad (7)$$

For high beta plasmas the dispersion relation is modified, specially for higher frequencies $\omega \sim kv_{\text{th}}$. For example, in the MHD regime, in addition to the Alfvén mode one gets fast and slow modes with the dispersion relation (see e.g. Sturrock 1994)

$$(\omega/k)^2 = \frac{1}{2} \left[(v_A^2 + v_s^2) \pm \sqrt{v_A^4 + v_s^4 - 2v_A^2 v_s^2 \cos 2\theta} \right], \quad (8)$$

and the more general dispersion relation (Eq. 5) is modified in a more complicated way (see e.g. André 1985 or Swanson 1989). The finite temperature imparts an imaginary part ω_i to the wave frequency that gives the damping rate $\Gamma(k)$ as long as $\omega_i < \omega_r$, the

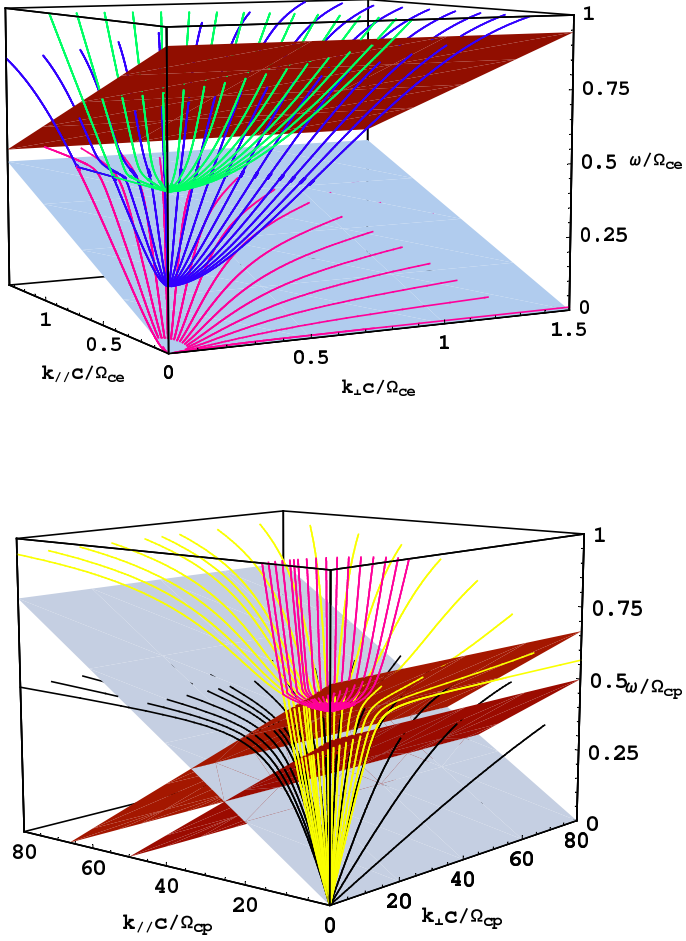


Fig. 1 Dispersion relation (curves) surfaces for a *cold* fully ionised H and He (10 % by number) plasma and resonance condition (flat) surfaces showing the regions around the electron (top panel) and proton (bottom panel) gyro-frequencies. Only waves with positive k_{\parallel}, k_{\perp} (or $0 < \theta < \pi/2$) are shown. The mirror image with respect to the (ω, k_{\perp}) plane gives the waves propagating in the opposite direction. From high to low frequencies, we have one of the electromagnetic branches (green), upper-hybrid branch (purple), lower-hybrid branch, which also includes the whistler waves (pink), fast-wave branches (yellow), and Alfvén branch (black). The effects of a finite temperature modify these curves at frequencies $\omega \sim kv_{th}$, where $v_{th} = \sqrt{2kT/m}$ is the thermal velocity (see e.g. André 1985). The resonance surfaces are for electrons with $v = 0.3c$ and $|\mu| = 1.0$ (top panel: upper, brown $n = 1$, lower, light blue $n = 0$) and ${}^4\text{He}$ (bottom panel: middle, brown $n = 1$) and ${}^3\text{He}$ (bottom panel: upper, brown $n = 1$) ions with $|\mu| = 1.0$ and $v = 0.01c$. The resonance surfaces for the latter two are the same when $n = 0$ (bottom panel: lower).

real part of the frequency⁵. For more details see e.g. Barnes & Scargle (1973); Swanson (1989); Pryadko & Petrosian (1998, 1999); Cranmer & Van Ballegoijen (2003); Brunetti & Lazarian (2007). In general, these rates and the modification of the dispersion relation are known for Maxwellian (sometimes anisotropic) energy distributions of the plasma particles. For non-thermal distributions the damping rates can be evaluated as described Petrosian et al. (2006) using the coupling described in Eq. 11 below.

2.3 Kinetic equations and their coefficients

2.3.1 Wave equation

Adopting the diffusion approximation (see e.g. Zhou & Matthaeus 1990), one can obtain the evolution of the spatially integrated wave spectrum $W(\mathbf{k}, t)$ from the general equation

$$\frac{\partial W}{\partial t} = \frac{\partial}{\partial k_i} \left[D_{ij} \frac{\partial}{\partial k_j} W \right] - \Gamma(\mathbf{k})W - \frac{W}{T_{\text{esc}}^W(\mathbf{k})} + \dot{Q}^W, \quad (9)$$

where \dot{Q}^W is the rate of generation of PWT at k_{min} , T_{esc}^W is the escape time, and D_{ij} and Γ describe the cascade and damping of the waves. The calculation of the damping rate is complicated but as described above it is well understood, but there are many uncertainties about the treatment of the cascade process or the form of D_{ij} . This is primarily because of incompleteness of the theoretical models and sufficient observational or experimental data. There are some direct observations in the Solar wind (e.g. Leamon et al. 1998) and indirect inferences in the interstellar medium (see e.g. Armstrong et al. 1995). There is some hope (Inogamov & Sunyaev, 2003) of future observations in the ICM. Attempts in fitting the Solar wind data have provided some clues about the cascade diffusion coefficients (see Leamon et al. 1999; Jiang et al. 2007).

2.3.2 Particle acceleration and transport

As described by Petrosian et al. 2008 - Chapter 10, this volume, the general equation for treatment of particles is the Fokker-Planck equation which for ICM conditions can be simplified considerably. As pointed out above we expect a short mean free path and fast scatterings for all particles. When the scattering time $\tau_{\text{scat}} = \lambda_{\text{scat}}/v \sim \langle 1/D_{\mu\mu} \rangle$ is much less than the dynamic and other timescales, the particles will have an isotropic pitch angle distribution. The pitch-angle averaged and spatially integrated particle distribution is obtained from⁶

$$\frac{\partial N(E, t)}{\partial t} = \frac{\partial}{\partial E} \left[D_{EE} \frac{\partial N(E, t)}{\partial E} - (A - \dot{E}_L)N(E, t) \right] - \frac{N(E, t)}{T_{\text{esc}}^P} + \dot{Q}^P. \quad (10)$$

Here D_{EE}/E^2 is the energy diffusion, due to scattering by PWT as described above and due to Coulomb collisions as discussed by Petrosian et al. 2008 - Chapter 10, this

⁵ Note that the 'thermal' effects change ω_r only slightly so that often the real part, the resonant interaction rate and the particle diffusion coefficients can be evaluated using the simpler cold plasma dispersion relation depicted in Fig. 1.

⁶ The derivation of this equation for the stated conditions and some other details can be found in the Appendix.

volume, $A(E)/E \sim \zeta D_{EE}/E^2$, with $\zeta(E) = (2 - \gamma^{-2})/(1 + \gamma^{-1})$ is the rate of direct acceleration due to interactions with PWT and all other agents, e.g., direct first order Fermi acceleration by shocks, \dot{E}_L/E is the energy loss rate of the particles (due to Coulomb collisions and synchrotron and IC losses, see Fig. 4 in Petrosian et al. 2008 - Chapter 10, this volume), and \dot{Q}^p and the term with the escape times T_{esc}^p describe the source and leakage of particles⁷.

The above two kinetic equations are coupled by the fact that the coefficients of one depend on the spectral distribution of the other; the damping rate of the waves depends on $N(E, t)$ and the diffusion and accelerations rates of particles depend on the wave spectrum $W(\mathbf{k}, t)$. Conservation of energy requires that the energy lost by the waves $\dot{W}_{\text{tot}} \equiv \int \Gamma(\mathbf{k})W(\mathbf{k})d^3k$ must be equal to the energy gained by the particles from the waves; $\dot{\mathcal{E}} = \int [A(E) - A_{\text{sh}}]N(E)dE$. Representing the energy transfer rate between the waves and particles by $\Sigma(\mathbf{k}, E)$ this equality implies that

$$\Gamma(\mathbf{k}) = \int_0^\infty dE N(E)\Sigma(\mathbf{k}, E), \quad A(E) = \int_0^\infty d^3k W(\mathbf{k})\Sigma(\mathbf{k}, E) + A_{\text{sh}}, \quad (11)$$

where we have added A_{sh} to represent contributions of other (non-stochastic acceleration) processes affecting the direct acceleration, e.g., shocks.

If the damping due to non-thermal particles is important then the wave and particle kinetic equations (9) and (10) are coupled and attempts have been made to obtain solutions of the coupled equations (Miller et al., 1996; Brunetti & Blasi, 2005). However, most often the damping rate is dominated by the background thermal particles so that the wave and non-thermal particle kinetic equations decouple. This is a good approximation in the ICM when dealing with relativistic electrons so that for determination of the particle spectra all we need is the boundaries of the inertial range ($k_{\text{min}}, k_{\text{max}}$), the wave spectral index q in this range (most likely $5/3 < q < 3/2$), and the shape of the spectrum above k_{max} which is somewhat uncertain (see Jiang et al. 2007).

3 Particle acceleration in clusters of galaxies

We now address the problem of particle acceleration in clusters of galaxies. The current information on the ICM does not allow us to treat the problem as outlined above by solving the coupled kinetic equations. In what follows we make reasonable assumptions about the turbulence and the particle diffusion coefficients, and then solve the particle kinetic equation to determine $N(E, t)$. We first consider the apparently simple scenario of acceleration of the background thermal particles. Based on some general arguments, Petrosian (2001, P01 hereafter) showed that this is not a viable mechanism. Here we carry out a more accurate calculation and show that this indeed is the case. This leads us to consider the transport and acceleration of high energy particles injected into the ICM by other processes.

⁷ in what follows we will assume that the waves are confined to the ICM so that $T_{\text{esc}}^W \rightarrow \infty$ and in some cases we will assume no escape of particles and let $T_{\text{esc}}^p \rightarrow \infty$.

3.1 Acceleration of background particles

The source particles to be accelerated are the ICM hot electrons subject to diffusion in energy space by turbulence and Coulomb collisions, acceleration by turbulence or shocks, and energy losses due to Coulomb collisions⁸. We start with an ICM of $kT = 8$ keV, $n = 10^{-3}$ cm⁻³ and assume a continuous injection of turbulence so that its density remains constant resulting in a time independent diffusion and acceleration rate. The results described below is from a recent paper by Petrosian & East (2007, PE07 hereafter). Following this paper we assume a simple but generic energy dependence of these coefficients. Specifically we assume a simple acceleration rate or timescale

$$\tau_{ac} = E/A(E) = \zeta D(E)/E^2 = \tau_0(1 + E_c/E)^p. \quad (12)$$

Fig. 2 shows a few examples of these time scales along with the effective Coulomb (plus IC and synchrotron) loss times as described in Fig. 3 of Petrosian et al. 2008 - Chapter 10, this volume.

We then use Eq. 10 to obtain the time evolution of the particle spectra. After each time step we use the resultant spectrum to update the Coulomb coefficients as described by Petrosian et al. 2008 - Chapter 10, this volume. At each step the electron spectrum can be divided into a quasi-thermal and a 'non-thermal' component. A best fit Maxwellian distribution to the quasi-thermal part is obtained, and we determine a temperature and the fraction of the thermal electrons. The remainder is labelled as the non-thermal tail. (For more details see PE07). The left and middle panels of Fig. 3 show two spectral evolutions for two different values of acceleration time $\tau_0/\tau_{Coul} = 0.013$ and 2.4, respectively, and for $E_c = 25$ keV and $p = 1$. The last spectrum in each case is for time $t = \tau_0$, corresponding to an equal energy input for all cases. The initial and final temperatures, the fraction of particles in the quasi-thermal component N_{th} , and the ratio of non-thermal to thermal energies R_{nonth} are shown for each panel. The general feature of these results is that the turbulence causes both acceleration and heating in the sense that the spectra at low energies resemble a thermal distribution but also have a substantial deviation from this quasi-thermal distribution at high energies which can be fitted by a power law over a finite energy range. The distribution is broad and continuous, and as time progresses it becomes broader and shifts to higher energies; the temperature increases and the non-thermal 'tail' becomes more prominent. There is very little of a non-thermal tail for $\tau_0 > \tau_{Coul}$ and most of the turbulent energy goes into heating (middle panel). Note that this also means that for a steady state case where the rate of energy gained from turbulence is equal to radiative energy loss rate (in this case thermal Bremsstrahlung, with time scale $\gg \tau_{Coul}$) there will be an insignificant non-thermal component. There is no distinct non-thermal tail except at unreasonably high acceleration rate (left panel). Even here there is significant heating (almost doubling of the temperature) within a short time ($\sim 3 \times 10^5$ yr). At such rates of acceleration most particles will end up at energies much larger than the initial kT and in a broad non-thermal distribution. We have also calculated spectra for different values of the cutoff energy E_c and index p . As expected for larger (smaller) values of E_c and smaller (higher) values of p the fraction of non-thermal particles is lower (higher).

⁸ In our numerical results we do include synchrotron, IC and Bremsstrahlung losses. But these have an insignificant effect in the case of nonrelativistic electrons under investigation here.

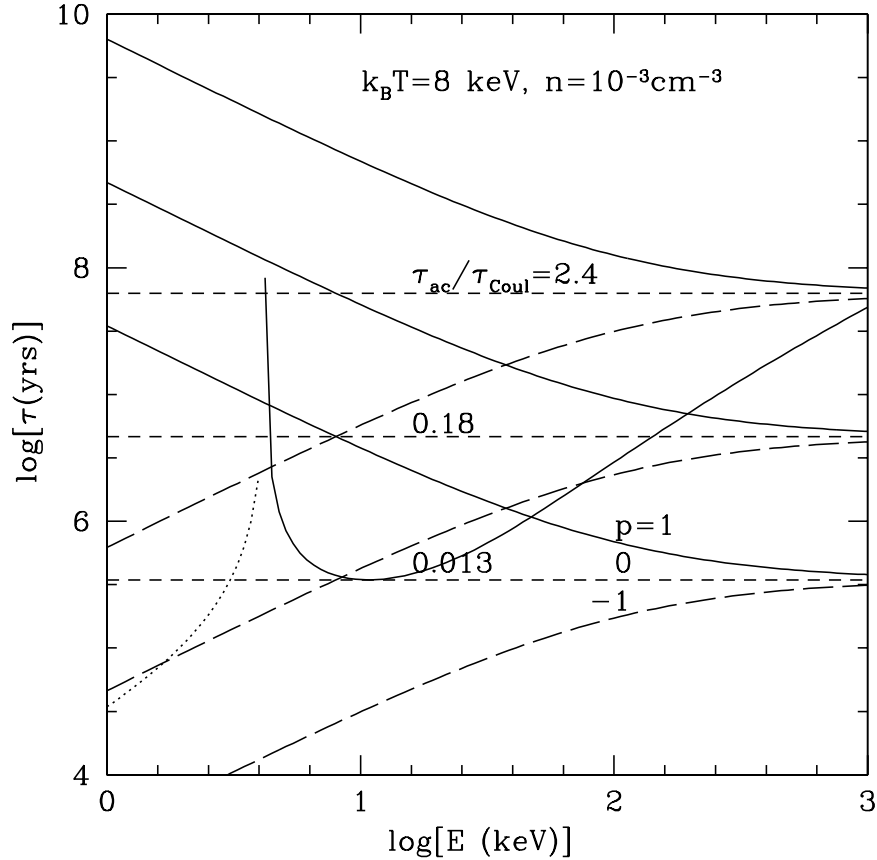


Fig. 2 Acceleration and loss timescales for ICM conditions based on the model described in the text. We use the effective Coulomb loss rate given by Petrosian et al. 2008 - Chapter 10, this volume, and the IC plus synchrotron losses for a CMB temperature of $T_{\text{CMB}} = 3$ K and an ICM magnetic field of $B = 1 \mu\text{G}$. We also use the simple acceleration scenario of Eq. 12 for $E_c = 0.2m_e c^2$ (~ 100 keV) and for the three specified values of p and times $\tau_0/\tau_{\text{Coul}}$ (from Petrosian & East 2007).

The evolution in time of the temperature (in units of its initial value), the fraction of the electrons in the 'non-thermal' component, the energy ratio R_{nonth} as well as an index $\delta = -d \ln N(E)/d \ln E$ for the non-thermal component are shown in the right panel of Fig. 3. All the characteristics described above are more clearly evident in this panel and similar ones for $p = -1$ and $+1$. In all cases the temperature increases by more than a factor of 2. This factor is smaller at higher rates of acceleration. In addition, high acceleration rates produce flatter non-thermal tails (smaller δ) and a larger fraction of non-thermal particles (smaller N_{th}) and energy (R_{nonth}).

It should be noted that the general aspects of the above behaviour are dictated by the Coulomb collisions and are fairly insensitive to the details of the acceleration mechanism which can affect the spectral evolution somewhat quantitatively but not its qualitative aspects. At low acceleration rates one gets mainly heating and at high

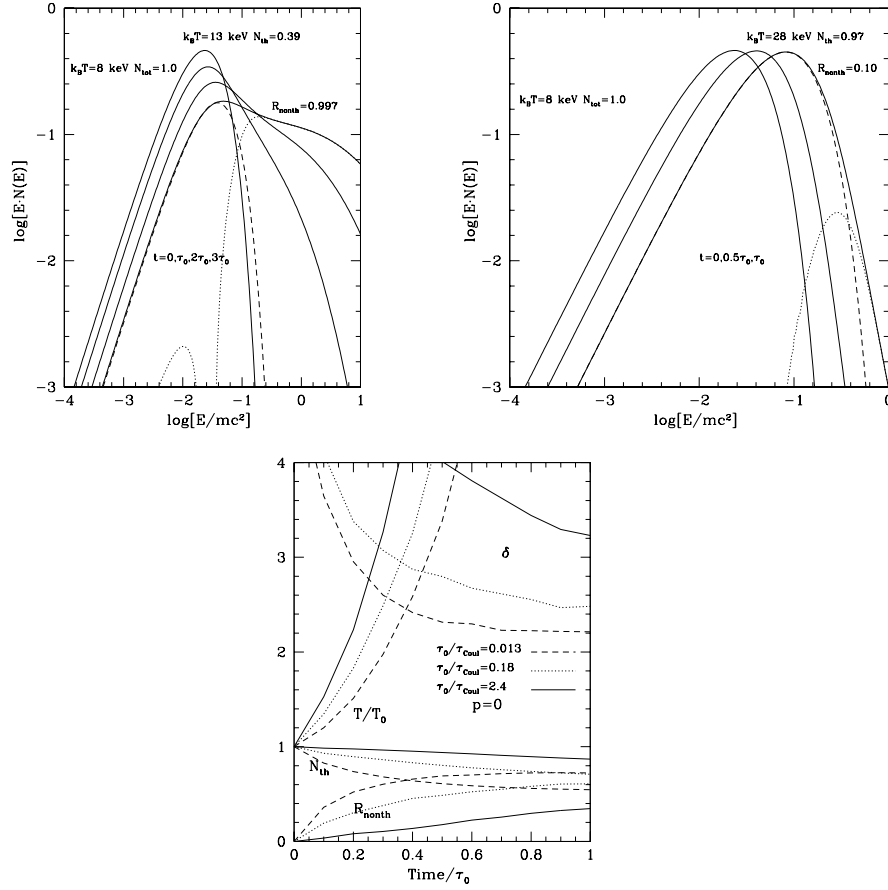


Fig. 3 *Upper left panel:* Evolution with time of electron spectra in the presence of a constant level of turbulence that accelerates electrons according to Eq. 12 with $\tau_0/\tau_{\text{Coul}} = 0.013$, $E_c = 0.2$ (~ 100 keV) and $p = 1$. For the last spectrum obtained for time $t = \tau_0$, the low end of the spectrum is fitted to a thermal component (dashed curve). The residual 'non-thermal' part is shown by the dotted curve. We also give the initial and final values of the temperature, the fraction of electrons in the thermal component N_{th} , and the ratio of energy of the non-thermal component to the thermal components R_{nonth} . *Upper right panel:* Same as above except for $\tau_0/\tau_{\text{Coul}} = 2.4$. Note that now there is only heating and not much of acceleration. *Lower panel:* Evolution with time (in units of τ_0) of electron spectral parameters, $T(t)/T_0$, N_{th} , R_{nonth} and the power-law index δ for indicated values of $\tau_0/\tau_{\text{Coul}}$ and for $p = 0$ and $E_c = 100$ keV. Note that for models with the same value of p at $t = \tau_0$ roughly the same amount of energy has been input into the ICM (from Petrosian & East 2007).

acceleration rate a prominent non-thermal tail is present but there is also substantial heating within one acceleration timescale which for such cases is very short. Clearly in a steady state situation there will be an insignificant non-thermal component. These findings support qualitatively findings by P01 and do not support the presence of distinct non-thermal tails advocated by Blasi (2000) and Dogiel et al. (2007), but agree

qualitatively with the more rigorous analysis of Wolfe & Melia (2006). For further results, discussions and comparison with earlier works see PE07.

We therefore conclude that the acceleration of background electrons stochastically or otherwise and non-thermal bremsstrahlung are not a viable mechanism for production of non-thermal hard X-ray excesses observed in some clusters of galaxies.

3.2 Acceleration of injected particles

The natural way to overcome the above difficulties is to assume that the radio and the hard X-ray radiation are produced by relativistic electrons injected in the ICM, the first via synchrotron and the second via the inverse Compton scattering of CMB photons. The energy loss rate of relativistic electrons can be approximated by (see P01)

$$\dot{E}_L(E)/E_p = (1 + (E/E_p)^2)/\tau_{\text{loss}}, \quad (13)$$

where

$$\tau_{\text{loss}} = E_p / (4\pi r_0^2 m_e c^3 n \ln \Lambda) \quad \text{and} \quad E_p \simeq m_e c^2 \left[\frac{9}{8} \frac{n \ln \Lambda}{u_{\text{ph}} + B^2/8\pi} \right]^{1/2} \quad (14)$$

are twice the loss time and the energy where the total loss curve reaches its maximum⁹ (see Fig. 4). Here $r_0 = e^2/(m_e c^2) = 2.82 \times 10^{-13}$ cm is the classical electron radius, u_{ph} (due to the CMB) and $B^2/8\pi$ are photon (primarily CMB) and magnetic field energy densities. For the ICM $B \sim \mu\text{G}$, $n = 10^{-3} \text{ cm}^{-3}$ and the Coulomb logarithm $\ln \Lambda = 40$ so that $\tau_{\text{loss}} = 6.3 \times 10^9$ yr and $E_p = 235 m_e c^2$.

The electrons are scattered and gain energy if there is some turbulence in the ICM. The turbulence should be such that it resonates with the injected relativistic electrons and not the background thermal nonrelativistic electrons for the reasons described in the previous section. Relativistic electrons will interact mainly with low wavevector waves in the inertial range where $W(k) \propto k^{-q}$ with the index $q \sim 5/3$ or $3/2$ for a Kolmogorov or Kraichnan cascade. There will be little interaction with nonrelativistic background electrons if the turbulence spectrum is cut off above some maximum wave vector k_{max} whose value depends on viscosity and magnetic field. The coefficients of the transport equation (Eq. 10) can then be approximated by

$$D(E) = \mathcal{D}E^q, \quad A(E) = a\mathcal{D}E^{q-1}, \quad \text{and} \quad T_{\text{esc}} = \mathcal{T}_{\text{esc}}E^s. \quad (15)$$

For a stochastic acceleration model at relativistic energies $a = 2$, but if in addition to scattering by PWT there are other agents of acceleration (e.g. shocks) then the coefficient a will be larger than 2. In this model the escape time is determined by the crossing time $T_{\text{cross}} \sim R/c$ and the scattering time $\tau_{\text{scat}} \sim D_{\mu\mu}^{-1}$. We can then write $T_{\text{esc}} \sim T_{\text{cross}}(1 + T_{\text{cross}}/\tau_{\text{scat}})$. Some examples of these are shown in Fig. 4. However, the escape time is also affected by the geometry of the magnetic field (e.g. the degree of its entanglement). For this reason we have kept the form of the escape time to be more general. In addition to these relations we also need the spectrum and rate of injection to obtain the spectrum of radiating electrons. Clearly there are several possibilities. We divided it into two categories: *steady state* and *time dependent*. In each case we first consider only the effects of losses, which means $\mathcal{D} = 0$ in the above expressions, and then the effects of both acceleration and losses.

⁹ We ignore the Bremsstrahlung loss and the weak dependence on E of Coulomb losses at nonrelativistic energies. We can also ignore the energy diffusion rate due to Coulomb scattering.

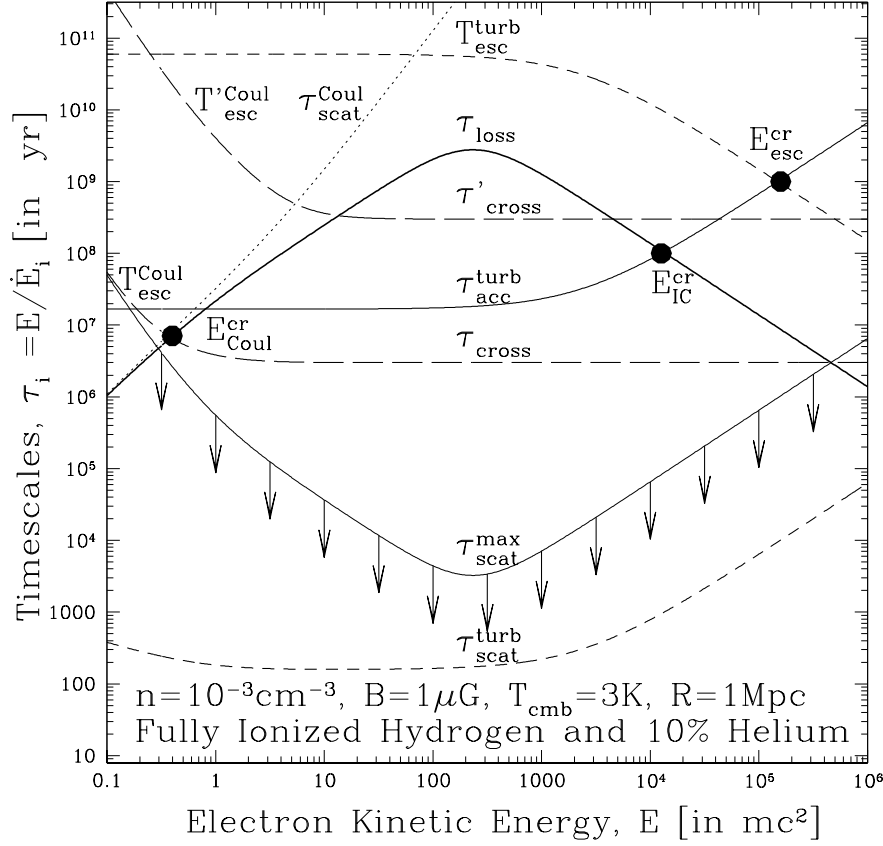


Fig. 4 Comparison of the energy dependence of the total loss time (radiative plus Coulomb; thick solid line) with timescales for scattering τ_{scat} (lower dashed line), acceleration τ_{ac} (thin solid lines), crossing time $\tau_{\text{cross}} \sim R/c\beta$ (long dashed lines) and escape time $T_{\text{esc}} \sim \tau_{\text{cross}}^2/\tau_{\text{scat}}$ (upper dashed line) of electrons. At low energies the scattering and escape times are dominated by Coulomb scattering but at high energies turbulence scattering becomes more important. The acceleration is constant at low energies ($A(E) \propto E$) but increases at high energies, corresponding to an acceleration rate $A(E) \rightarrow$ a constant at high E or to a turbulence spectral index $q = 1$. A chaotic magnetic field with scale of 10 kpc will increase the crossing time to the primed curve. The arrows show the maximum scattering times for which the escape times are equal or longer than the total loss times. The critical energies where the acceleration time is equal to the escape time, the Coulomb and inverse Compton loss times are shown.

3.2.1 Steady state cases

By steady state we mean variation timescales of order or larger than the Hubble time which is also longer than the maximum loss time $\tau_{\text{loss}}/2$. Given a particle injection rate $\dot{Q} = \dot{Q}_0 f(E)$ (with $\int f(E) dE = 1$) steady state is possible if $\mathcal{T}_{\text{esc}} = \dot{Q}_0 / \int N(E) E^{-s} dE$.

In the absence of acceleration ($\mathcal{D} = 0$) eQ. 10 can be solved analytically. For the examples of escape times given in Fig. 4 ($T_{\text{esc}} > \tau_{\text{loss}}$) one gets the simple cooling

spectra $N = (\dot{Q}\tau_{\text{loss}}/E_p) \int_E^\infty f(E)dE/(1 + (E/E_p)^2)$, which gives a spectral index break at E_p from index $p_0 - 1$ below to $p_0 + 1$ above E_p , for an injected power law $f(E) \propto E^{-p_0}$. For $p_0 = 2$ this will give a high energy power law in rough agreement with the observations but with two caveats. The first is that the spectrum of the injected particles must be cutoff below $E \sim 100m_e c^2$ to avoid excessive heating and the second is that this scenario cannot produce the broken power law or exponential cutoff we need to explain the radio spectrum of Coma (see Fig. 6 and the discussion in Petrosian et al. 2008 - Chapter 10, this volume). A break is possible only if the escape time is shorter than τ_0 in which case the solution of the kinetic equation for a power law injected spectrum ($p_0 > 1$ and $s > -1$) leads to the broken power law

$$N(E) = Q_0 \begin{cases} \mathcal{T}_{\text{esc}}(E/E_p)^{-p_0+s} & \text{if } E \ll E_{\text{cr}}, \\ \tau_{\text{loss}}(E/E_p)^{-p_0-1}/(s+1) & \text{if } E_{\text{cr}} \ll E, \end{cases} \quad (16)$$

where $E_{\text{cr}} = E_p((s+1)(\mathcal{T}_{\text{esc}}/\tau_{\text{loss}}))^{-1/(s+1)}$. Thus, for $p_0 \sim 3$ and $s = 0$ and $T_{\text{esc}} \simeq 0.02\tau_{\text{loss}}$ we obtain a spectrum with a break at $E_{\text{cr}} \sim 10^4$, in agreement with the radio data (Rephaeli 1979 model). However, this also means that a large fraction of the $E < E_p$ electrons escape from the ICM, or more accurately from the turbulent confining region, with a flux of $F_{\text{esc}}(E) \propto N(E)/T_{\text{esc}}(E)$. Such a short escape time means a scattering time which is only ten times shorter than the crossing time and a mean free path of about $\sim 0.1R \sim 100$ kpc. This is in disagreement with the Faraday rotation observations which imply a tangled magnetic field equivalent to a ten times smaller mean free path. The case for a long escape time was first put forth by Jaffe (1977).

Thus it appears that in addition to injection of relativistic electrons we also need a steady presence or injection of PWT to further scatter and accelerate the electrons. The final spectrum of electrons will depend on the acceleration rate and its energy dependence. In general, when the acceleration is dominant one expects a power law spectrum. Spectral breaks appear at critical energies when this rate becomes equal to and smaller than other rates such as the loss or escape rates (see Fig. 4). In the energy range where the losses can be ignored electrons injected at energy E_0 ($f(E) = \delta(E - E_0)$) one expects a power law above (and below, which we are not interested in) this energy. In the realistic case of long T_{esc} (and/or when the direct acceleration rate is larger than the rate of stochastic acceleration (i.e. $a \gg 1$) then spectral index of the electrons will be equal to $-q + 1$ requiring a turbulence spectral index of $q = 4$ which is much larger than expected values of $5/3$ or $3/2$ (see Park & Petrosian 1995). This spectrum will become steeper (usually cut off exponentially) above the energy where the loss time becomes equal to the acceleration time $\tau_{\text{ac}} = E/A(E)$ or at $E_{\text{cr}} = (E_p a \mathcal{D} \tau_{\text{loss}})^{1/(3-q)}$. Steeper spectra below this energy are possible only for shorter T_{esc} . The left panel of Fig. 5 shows the dependence of the spectra on T_{esc} for $q = 2$ and $s = 0$ (acceleration and escape times independent of E). The spectral index just above E_0 is $p = \sqrt{9/4 + 2\tau_{\text{ac}}/T_{\text{esc}}} - 1.5$. In the limit when $T_{\text{esc}} \rightarrow \infty$ the distribution approaches a relativistic Maxwellian distribution $N \propto E^2 e^{-E/E_{\text{cr}}}$. For a cut-off energy $E_{\text{cr}} \sim 10^4$ this requires an acceleration time of $\sim 10^8$ yr and for a spectral index of $p = 3$ below this energy we need $T_{\text{esc}} \sim \tau_{\text{ac}}/18 \sim 5 \times 10^6$ yr which is comparable to the unhindered crossing time. This is too short. As shown in Fig. 4 any scattering mean free path (or magnetic field variation scale) less than the cluster size will automatically give a longer escape time and a flatter than required spectrum. For further detail on all aspects of this case see Park & Petrosian (1995), P01 and Liu et al. (2006).

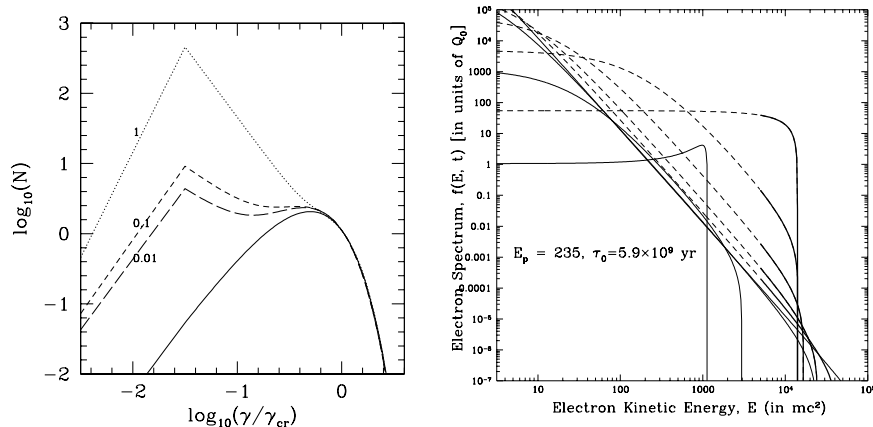


Fig. 5 *Left panel:* The steady state electron spectra injected at energy E_0 and subject to continuous acceleration by turbulence with spectral index $q = 2$ for different values of the ratio $T_{\text{esc}}/\tau_{\text{loss}}$. Note that τ_0 in the label is the same as τ_{loss} in the text. For very high values of this ratio we get a relativistic Maxwellian distribution (from Liu et al. 2006). *Right panel:* Evolution with time of a power law injected spectrum (top line) subject to Coulomb and inverse Compton (plus synchrotron) losses as given by Eq. 17. Solid lines for $b = 2$ ($t/\tau_0 = 10^{-n}$; $n = 3, 2, 1, 0$), and dashed lines for $b = 60$ ($t/\tau_0 = 10^{-2.18+n/3}$; $n = 0, 1, 2, 3, 4$). The heavy portions show the energy range of the electrons needed for production of radio and hard X-rays.

In summary there are several major difficulties with the steady state model.

3.2.2 Time dependent models

We are therefore led to consider time dependent scenarios with time variation shorter than the Hubble time. The time dependence may arise from the episodic nature of the injection process (e.g. varying AGN activity) and/or from episodic nature of turbulence generation process (see e.g. Cassano & Brunetti 2005). In this case we need solutions of the time dependent equation (Eq. 10). We start with the generic model of a prompt single-epoch injection of electrons with $Q(E, t) = Q(E)\delta(t - t_0)$. More complex temporal behaviour can be obtained by the convolution of the injection time profile with the solutions described below. The results presented below are from P01. Similar treatments of the following cases can be found in Brunetti et al. (2001) and Brunetti & Lazarian (2007).

It is clear that if there is no re-acceleration, electrons will lose energy first at highest and lowest energies due to inverse Compton and Coulomb losses, respectively. Particles will be peeled away from an initial power law with the low and high energy cut-offs moving gradually toward the peak energy E_p . A more varied and complex set of spectra can be obtained if we add the effects of diffusion and acceleration. Simple analytic solutions for the time dependent case are possible only for special cases. Most of the complexity arises because of the diffusion term which plays a vital role in shaping the spectrum for a narrow injection spectrum. For some examples see Park & Petrosian (1996). Here we limit our discussion to a broad initial electron spectrum in which case the effects of this term can be ignored until such features are developed. Thus, if we set $D(E) = 0$, which is a particularly good approximation when $a \gg 1$, and for the

purpose of demonstration if we again consider the simple case of constant acceleration time ($q = 2$ and $A(E) = aDE$), then the solution of Eq. 10 gives

$$N(E, t) = \exp\{-t/T_{\text{esc}}\} Q_0 \frac{[T_+ - (E/E_p) \tan(\delta t/\tau_{\text{loss}})/\delta]^{p_0-2}}{\cos^2(\delta t/\tau_{\text{loss}})[T_- (E/E_p) + \tan(\delta t/\tau_{\text{loss}})/\delta]^{p_0}}, \quad (17)$$

where $\delta^2 = 1 - b^2/4$, $b = aD\tau_0 E_p^2 = \tau_{\text{loss}}/\tau_{\text{ac}}$ and $T_{\pm} = 1 \pm b \tan(\delta t/\tau_{\text{loss}})/(2\delta)$. Note that $b = 0$ correspond to the case of no acceleration described above. This solution is valid for $b^2 < 4$. For $b^2 > 4$ we are dealing with an imaginary value for δ so that tangents and cosines become hyperbolic functions with $\delta^2 = b^2/4 - 1$. For $\delta = 0$ or $b = 2$ this expression reduces to

$$N(E, t) = \exp\{-t/T_{\text{esc}}\} Q_0 \frac{[1 - (E/E_p - 1)t/\tau_{\text{loss}}]^{p_0-2}}{[E/E_p - (E/E_p - 1)t/\tau_{\text{loss}}]^{p_0}}. \quad (18)$$

The right panel of Fig. 5 shows the evolution of an initial power law spectrum subjected to weak acceleration ($b = 2$, solid lines) and a fairly strong rate of acceleration ($b = 60$, dashed line). As expected with acceleration, one can push the electron spectra to higher levels and extend it to higher energies. At low rates of acceleration the spectrum evolves toward the generic case of a flat low energy part with a fairly steep cutoff above E_p . At higher rates, and for some periods of time comparable to τ_{ac} , the cut off energy E_{cr} will be greater than E_p and there will be a power law portion below it.¹⁰ As evident from this figure there are periods of time when in the relevant energy range (thick solid lines) the spectra resemble what is needed for describing the radio and hard X-ray observations from Coma described in Fig. 6 of Petrosian et al. 2008 - Chapter 10, this volume.

In summary, it appears that a steady state model has difficulties and that the most likely scenario is episodic injection of relativistic particles and/or turbulence and shocks which will re-accelerate the existing or injected relativistic electrons into a spectral shape consistent with observations. However these spectra are short lived, lasting for periods of less than a billion years.

4 Summary and conclusion

We have given a brief overview of particle acceleration in astrophysical plasmas in general, and acceleration of electrons in the ICM in particular. We have pointed out the crucial role plasma waves and turbulence play in all acceleration mechanisms and outlined the equations that describe the generation, cascade and damping of these waves and the coupling of these processes to the particle kinetics and energising of the plasma and acceleration in both relativistic and nonrelativistic regimes.

We have applied these ideas to the ICM of clusters of galaxies with the aim of production of electron spectra which can explain the claimed hard X-ray emission either as non-thermal bremsstrahlung emission by nonrelativistic electrons or as inverse Compton emission via scattering of CMB photons by a population of relativistic electrons. It is shown that the first possibility which can come about by accelerating background electrons into a non-thermal tail is not a viable mechanism, as was pointed earlier in

¹⁰ At even later times than shown here one gets a large pile up at the cut off energy (see P01). This latter feature is of course artificial because we have neglected the diffusion term which will smooth out such features (see Brunetti & Lazarian 2007).

P01. The primary reason for this difficulty is due to the short Coulomb collision and loss timescales. Quite generally, it can be stated that at low rates of acceleration one obtains a hotter plasma and an insignificant non-thermal tail. Discernible tails can be obtained at higher rates of acceleration but only for short periods of time. For periods on the order of a billion year such rates will also cause excessive heating and will lead to runaway conditions where most of the electrons are accelerated to relativistic energies, at which they are no longer bound to the cluster, unless there exists a strong scattering agent.

This leads us to the model where hard X-rays are produced by the inverse Compton process and relativistic electrons. Moreover, even if the hard X-ray radiation turns out to be not present, or one finds a way to circumvent the above difficulties, we still require the presence of relativistic electrons to explain the radio emission. These electrons must be injected into the ICM by some other means. They can come from galaxies, specially when they are undergoing an active nuclear (or AGN) phase. Or they may be due to interactions of cosmic ray protons with thermal protons and the resultant pion decays. We have shown that just injection may not be sufficient, because for reasonable injected spectra the transport effects in the ICM modify the spectrum such that the effective radiating spectrum is inconsistent with what is required. Thus, a re-acceleration in the ICM is necessary and turbulence and merger shocks may be the agent of this acceleration. In this case, it also appears that a steady state scenario, like the hadronic mechanism described above, will in general give a flatter than required spectrum unless the electrons escape the ICM unhindered. This requirement is not reasonable because the expected tangled magnetic field will increase this time. But, more importantly, the presence of turbulence necessary for re-acceleration will result in a short mean free path and a much longer escape time.

A more attractive scenario is if the injection of electrons and/or the production of turbulence is episodic. For example for a short lived electron injected phase (from say an AGN) but a longer period of presence of turbulence one can determine the spectral evolution of the electrons subject to acceleration and losses. We have shown that for some periods of time lasting several times the acceleration timescales one can obtain electron spectra consistent with what is required by observations. The same will be true for a hadronic source if there is a short period of production of turbulence. In either case we are dealing with periods on the order of several hundreds of million years to a billion years, which is comparable with timescales expected from merging of Mpc size clusters with velocities of several thousands of km s^{-1} which are theoretically reasonable and agree with observations (see e.g. Bradač et al. 2006).

Acknowledgements The authors thank ISSI (Bern) for support of the team “Non-virialized X-ray components in clusters of galaxies”. A.M. B. acknowledges the RBRF grant 06-02-16844 and a support from RAS Programs.

A Particle kinetic equations

In this section we describe some of the mathematical details required for investigation of the acceleration and transport of all charged particles stochastically and by shocks, and the steps and conditions that lead to the specific kinetic equations (Eq. 10) used in this and the previous chapters.

A.1 Stochastic acceleration by turbulence

In strong magnetic fields, the gyro-radii of particles are much smaller than the scale of the spatial variation of the field, so that the gyro-phase averaged distribution of the particles depends only on four variables: time, spatial coordinate z along the field lines, the momentum p , and the pitch angle $\cos \mu$. In this case, the evolution of the particle distribution, $f(t, z, p, \mu)$, can be described by the Fokker-Planck equation as they undergo stochastic acceleration by interaction with plasma turbulence (diffusion coefficients D_{pp} , $D_{\mu\mu}$ and $D_{p\mu}$), direct acceleration (with rate \dot{p}_G), and suffer losses (with rate \dot{p}_L) due to other interactions with the plasma particles and fields:

$$\begin{aligned} \frac{\partial f}{\partial t} + v\mu \frac{\partial f}{\partial z} &= \frac{1}{p^2} \frac{\partial}{\partial p} p^2 \left[D_{pp} \frac{\partial f}{\partial p} + D_{p\mu} \frac{\partial f}{\partial \mu} \right] \\ &+ \frac{\partial}{\partial \mu} \left[D_{\mu\mu} \frac{\partial f}{\partial \mu} + D_{\mu p} \frac{\partial f}{\partial p} \right] \\ &- \frac{1}{p^2} \frac{\partial}{\partial p} [p^2 (\dot{p}_L - \dot{p}_G) f] \\ &+ J. \end{aligned} \quad (19)$$

Here βc is the velocity of the particles and $J(t, z, p, \mu)$ is a source term, which could be the background plasma or some injected spectrum of particles. The kinetic coefficients in the Fokker-Planck equation can be expressed through correlation functions of stochastic electromagnetic fields (see e.g. Melrose 1980; Berezhinskii et al. 1990; Schlickeiser 2002). The effect of the mean magnetic field convergence or divergence can be accounted for by adding

$$\frac{c\beta d \ln B}{ds} \frac{\partial}{\partial \mu} \left(\frac{(1 - \mu^2)}{2} f \right) \quad (20)$$

to the right hand side.

Pitch-angle isotropy: At high energies and in weakly magnetised plasmas with Alfvén velocity $\beta_A \equiv v_A/c \ll 1$ the ratio of the energy and pitch angle diffusion rates $D_{pp}/p^2 D_{\mu\mu} \approx (\beta_A/\beta)^2 \ll 1$, and one can use the *isotropic approximation* which leads to the *diffusion-convection equation* (see e.g. Dung & Petrosian 1994; Kirk et al. 1988):

$$F(z, t, p) \equiv \frac{1}{2} \int_{-1}^1 d\mu f(t, z, p, \mu), \quad \dot{Q}(t, z, p) \equiv \frac{1}{2} \int_{-1}^1 d\mu J(\mu, z, t, p), \quad (21)$$

$$\begin{aligned} \frac{\partial F}{\partial t} - \frac{\partial}{\partial z} \kappa_1 \frac{\partial F}{\partial z} &= (pv) \frac{\partial \kappa_2}{\partial z} \frac{\partial F}{\partial p} \\ &- \frac{1}{p^2} \frac{\partial}{\partial p} (p^3 v \kappa_2) \frac{\partial F}{\partial z} \\ &+ \frac{1}{p^2} \frac{\partial}{\partial p} \left(p^4 \kappa_3 \frac{\partial F}{\partial p} - p^2 \dot{p}_L F \right) \\ &+ \dot{Q}(z, t, p), \end{aligned} \quad (22)$$

$$\begin{aligned} \kappa_1 &= \frac{v^2}{8} \int_{-1}^1 d\mu \frac{(1 - \mu^2)^2}{D_{\mu\mu}}, \\ \kappa_2 &= \frac{1}{4} \int_{-1}^1 d\mu (1 - \mu^2) \frac{D_{\mu p}}{p D_{\mu\mu}}, \\ \kappa_3 &= \frac{1}{2} \int_{-1}^1 d\mu (D_{pp} - D_{\mu p}^2 / D_{\mu\mu}) p^2. \end{aligned}$$

At low energies, as shown by Pryadko & Petrosian (1997), specially for strongly magnetised plasmas ($\alpha \ll 1, \beta_A > 1$), $D_{pp}/p^2 \gg D_{\mu\mu}$, and then stochastic acceleration is more efficient than acceleration by shocks ($D_{pp}/p^2 \gg \dot{p}_G$). In this case the pitch angle dependence may not be ignored.

$$\frac{\partial f^\mu}{\partial t} + v\mu \frac{\partial f^\mu}{\partial z} = \frac{1}{p^2} \frac{\partial}{\partial p} p^2 D_{pp}^\mu \frac{\partial f^\mu}{\partial p} - \frac{1}{p^2} \frac{\partial}{\partial p} [p^2 \dot{p}_L f^\mu] + j^\mu, \quad (23)$$

However, Petrosian & Liu (2004) find that these dependences are in general weak and one can average over the pitch angles.

A.2 Acceleration in large scale turbulence and shocks

In an astrophysical context it often happens that the energy is released at scales much larger than the mean free path of energetic particles. If the produced large scale MHD turbulence is supersonic and superalfvénic then MHD shocks are present in the system. The particle distribution within such a system is highly intermittent. Statistical description of intermittent systems differs from the description of homogeneous systems. There are strong fluctuations of particle distribution in shock vicinities. A set of kinetic equations for the intermittent system was constructed by Bykov & Toptygin (1993), where the smooth averaged distribution obeys an integro-differential equation (due to strong shocks), and the particle distribution in the vicinity of a shock can be calculated once the averaged function was found.

The pitch-angle averaged distribution function $N(\mathbf{r}, p, t)$ of non-thermal particles (with energies below some hundreds of GeV range in the cluster case) averaged over an ensemble of turbulent motions and shocks satisfies the kinetic equation

$$\frac{\partial f}{\partial t} - \frac{\partial}{\partial r_\alpha} \chi_{\alpha\beta} \frac{\partial f}{\partial r_\beta} = G \hat{L} f + \frac{1}{p^2} \frac{\partial}{\partial p} p^4 D \frac{\partial f}{\partial p} + A \hat{L}^2 N + 2B \hat{L} \hat{P} f + \hat{J}(p), \quad (24)$$

The source term $\hat{J}(t, r, p)$ is determined by injection of particles. The integro-differential operators \hat{L} and \hat{P} are given by

$$\hat{L} = \frac{1}{3p^2} \frac{\partial}{\partial p} p^{3-\gamma} \int_0^p dp' p'^\gamma \frac{\partial}{\partial p'}; \quad \hat{P} = \frac{p}{3} \frac{\partial}{\partial p}. \quad (25)$$

The averaged kinetic coefficients A, B, D, G , and $\chi_{\alpha\beta} = \chi \delta_{\alpha\beta}$ are expressed in terms of the spectral functions that describe correlations between large scale turbulent motions and shocks, the particle spectra index γ depends on the shock ensemble properties (see Bykov & Toptygin 1993). The kinetic coefficients satisfy the following renormalisation equations:

$$\chi = \kappa_1(p) + \frac{1}{3} \int \frac{d^3 \mathbf{k} d\omega}{(2\pi)^4} \left[\frac{2T + S}{i\omega + k^2 \chi} - \frac{2k^2 \chi S}{(i\omega + k^2 \chi)^2} \right], \quad (26)$$

$$D = \frac{\chi}{9} \int \frac{d^3 \mathbf{k} d\omega}{(2\pi)^4} \frac{k^4 S(k, \omega)}{\omega^2 + k^4 \chi^2}, \quad (27)$$

$$A = \chi \int \frac{d^3 \mathbf{k} d\omega}{(2\pi)^4} \frac{k^4 \tilde{\phi}(k, \omega)}{\omega^2 + k^4 \chi^2}, \quad (28)$$

$$B = \chi \int \frac{d^3 \mathbf{k} d\omega}{(2\pi)^4} \frac{k^4 \tilde{\mu}(k, \omega)}{\omega^2 + k^4 \chi^2}. \quad (29)$$

Here $G = (1/\tau_{\text{sh}} + B)$. $T(k, \omega)$ and $S(k, \omega)$ are the transverse and longitudinal parts of the Fourier components of the turbulent velocity correlation tensor. Correlations between velocity jumps on shock fronts are described by $\tilde{\phi}(k, \omega)$, while $\tilde{\mu}(k, \omega)$ represents shock-rarefaction correlations. The introduction of these spectral functions is dictated by the intermittent character of a system with shocks.

The test particle calculations showed that the low energy branch of the particle distribution would contain a substantial fraction of the free energy of the system after a few acceleration times. Thus, to calculate the efficiency of the shock turbulence power conversion

to the non-thermal particle component, as well as the particle spectra, we have to account for the backreaction of the accelerated particles on the shock turbulence. To do that, Bykov (2001) supplied the kinetic equations Eqs. 24)–(29 with the energy conservation equation for the total system including the shock turbulence and the non-thermal particles, resulting in temporal evolution of particle spectra.

References

- Akhiezer, A.I., Akhiezer, I.A., Polovin, R.V., Sitenko, A.G., & Stepanov, K.N., 1975, *Plasma electrodynamics*, Pergamon Press, Oxford
- Amato, E., & Blasi, P., 2006, *MNRAS*, 371, 1251
- André, M., 1985, *J. Plasma Phys.*, 33, 1
- Armstrong, J.W., Rickett, B.J., & Spangler, S.R., 1995, *ApJ*, 443, 209
- Barnes, A., & Scargle, J.D., 1973, *ApJ*, 184, 251
- Bell, A.R., & Lucek, S.G., 2001, *MNRAS*, 321, 433
- Berezinskii, V.S., Bulanov, S.V., Dogiel, V.A., & Ptuskin, V.S., 1990, *Astrophysics of cosmic rays*, (North-Holland, Amsterdam)
- Blandford, R.d, & Eichler, D., *Phys. Rep.*, 154, 1
- Blandford, R.D., & Ostriker, J.P., 1978, *ApJ*, 221, L29
- Blasi, P., 2000, *ApJ*, 532, L9
- Boris, J.P., Dawson, J.M., Orens, J.H., & Roberts, K.V., 1970, *Phys. Rev. Lett.*, 25, 706
- Bradač, M., Clowe, D., Gonzalez, A.H., et al., 2006, *ApJ*, 652, 937
- Brunetti, G., & Blasi, P., 2005, *MNRAS*, 363, 1173
- Brunetti, G., & Lazarian, A., 2007, *MNRAS*, 378, 245
- Brunetti, G., Setti, G., Feretti, L., & Giovannini, G., 2001, *MNRAS* 320, 365
- Bykov, A.M., 2001, *SSR*, 99, 317
- Bykov, A.M. & Toptygin, I.N., 1993, *Physics Uspekhi*, 36, 1020
- Bykov, A.M., Bloemen, H. & Uvarov, Yu.A., 2000, *A&A*, 362, 886
- Bykov, A.M., Dolag, K., & Durret, F., 2008, *SSR*, in press
- Cassak, P.A., Drake, J.F., & Shay, M.A., 2006, *ApJ*, 644, L145
- Cassano, R., & Brunetti, G., 2005, *MNRAS* 357, 1313
- Chandran, B., 2005, *Phys. Rev. Lett.*, 95, 265004
- Cho, J., & Lazarian, A., 2002, *Phys. Rev. Lett.*, 88, 245001
- Cho, J., & Lazarian, A., 2006, *ApJ*, 638, 811
- Cranmer, S.R., & van Ballegoijen, A.A., 2003, *ApJ*, 594, 573
- Dogiel, V.A., Ko, C.M., Kuo, P.H., et al., 2007, *A&A*, 461, 433
- Dolag, K., Vazza, F., Brunetti, G., & Tormen, G., 2005, *MNRAS*, 364, 753
- Drake, J.F., 2006, Paper presented at Krakow Conference on Relativistic Jets, <http://www.oa.uj.edu.pl/2006jets/talks/Drake/Drake.pdf>
- Drury, L.Oc., 1983, *Rep. Progr. Phys.*, 46, 973
- Dung, R., & Petrosian, V., 1994, *ApJ*, 421, 550
- Durret, F., Kaastra, J.S., Nevalainen, J., Ohashi, T., & Werner, N., 2008, *SSR*, in press
- Ellison, D.C., Moebius, E., & Paschmann, G., 1990, *ApJ*, 352, 376
- Ellison, D.C., Decourchelle, A, & Ballet, J., 2005, *A&A*, 429, 569
- Ferrari, C., Govoni, F., Schindler, S., Bykov, A.M., & Rephaeli, Y., 2008, *SSR*, in press
- Goldreich, P., & Sridhar, S., 1995, *ApJ*, 438, 763
- Goldreich, P., & Sridhar, S., 1997, *ApJ*, 485, 680
- Holman, G.D., 1985, *ApJ*, 293, 584
- Inogamov, N.A. & Sunyaev, R.A., 2003, *Ast. Letters*, 29, 791
- Jaffe, W.J., 1977, *ApJ*, 212, 1
- Jiang, Y.W., et al. 2007, in preparation
- Jones, F.C., 1994, *ApJS*, 90, 561
- Jones, F.C., & Ellison, D.C., 1991, *SSR*, 58, 259
- Kennel, C.F., Coroniti, F.V., Scarf F.L., et al., 1986, *JGR*, 91, 11917
- Kirk, J.G., Schneider, P., & Schlickeiser, R. 1988, *ApJ*, 328, 269
- Leamon, R.J., Smith, C.W., Ness, N.F., Matthaeus, W.H., & Wong, H.K., 1998, *JGR*, 103, 4775
- Leamon, R.J., Smith, C.W., Ness, N.F., & Wong, H.K., 1999, *JGR*, 104, 22331
- Lithwick, Y., & Goldreich, P., 2003, *ApJ*, 582, 1220

-
- Liu, S., Melia, F., & Petrosian, V., 2006, *ApJ*, 636, 798
Luo, Q., & Melrose, D.B., 2006, *MNRAS*, 368, 115
Malkov, M.A., & Drury, L.O., 2001, *Rep. Progr. Phys.*, 64, 429
Melrose, D.B., 1980, *Plasma astrophysics* (Gordon and Breach, New York)
Miller, J.A., LaRosa, T.N., & Moore, R.L., 1996, *ApJ*, 461, 445
Park, B.T., & Petrosian, V., 1995, *ApJ*, 446, 699
Park, B.T., & Petrosian, V., 1996, *ApJS*, 103, 255
Petrosian, V., 2001, *ApJ*, 557, 560 (P01)
Petrosian, V., & East, W., 2007, *ApJ*, in press (PE07)
Petrosian, V., & Liu, S., 2004, *ApJ*, 610, 550
Petrosian, V., Yan, H. & Lazarian, A. 2006, *ApJ*, 644, 603
Petrosian, V., Bykov, A.M., & Rephaeli, Y., 2008, *SSR*, in press
Pryadko, J., & Petrosian, V., 1997, *ApJ*, 482, 774
Pryadko, J., & Petrosian, V., 1998, *ApJ*, 495, 377
Pryadko, J., & Petrosian, V., 1999, *ApJ*, 515, 873
Rephaeli, Y., 1979, *ApJ*, 227, 364
Rephaeli, Y., Nevalainen, J., Ohashi, T., & Bykov, A., 2008, *SSR*, in press
Ricker P.M., & Sarazin, C.L., 2001, *ApJ*, 561, 621
Roettiger, K., Burns, J.O., & Loken, C., 1996, *ApJ*, 473, 561
Schekochihin, A.A., Cowley, S.C., Kulsrud, R.M., Hammett, G.W., & Sharma, P., 2005, *ApJ*, 626, 139
Schlickeiser, R., 2002, *Cosmic ray astrophysics* (Springer, Berlin)
Schlickeiser, R., Campeanu, A., & Lerche, L., 1993, *A&A*, 276, 614
Sunyaev, R.A., Norman, M.L., & Bryan, G.L., 2003, *Astron. Lett.*, 29, 783
Swanson, D.G., 1989, *Plasma Waves* (Academic Press, New York)
Sturrock, P.A., 1994, *Plasma Physics* (Cambridge Univ. Press)
Vladimirov, A., Ellison, D.C., & Bykov, A., 2006, *ApJ*, 652, 1246
Vogt, C., & Enßlin, T.A., 2005, *A&A*, 434, 67
Völk, H.J., Berezhko, E.G., & Ksenofontov, L.T., 2005, *A&A*, 433, 229
Wolfe, B., & Melia, F., 2006, *ApJ*, 638, 125
Zenitani, S., & Hoshino, M., 2005, *ApJ*, 618, L111
Zhou, Y., & Matthaeus, W.H., 1990, *JGR*, 95, 14881